

# Structures of the formic acid trimer

Amlan K. Roy, Ajit J. Thakkar \*

*Department of Chemistry, University of New Brunswick, Fredericton, New Brunswick, Canada E3B 6E2*

Received 26 November 2003; in final form 5 January 2004

Published online: 7 February 2004

## Abstract

Hybrid density functional calculations are used to locate 33 local minima on the potential energy surface of the formic acid trimer. Additional computations are performed for the 14 lowest-energy structures to assess their sensitivity to enlarging the basis set and to varying the density functional. Energies and enthalpies show that the global minimum is a planar structure consisting of the lowest-energy dimer bound to the third monomer by a strong O–H···O bond. However, a planar, symmetric ring structure has the lowest Gibbs free energy.

© 2004 Elsevier B.V. All rights reserved.

## 1. Introduction

Formic acid, the simplest carboxylic acid, is of particular interest, and its importance in theoretical and experimental research is comparable to that of methanol or even water. Formic acid is present in clouds and fog, and plays an important role in human metabolism. Formic acid is one of the simplest molecules to exhibit rotational isomerism. The dimers of formic acid are prototypical models for multiple proton transfer reactions in which the constituents are held together by strong hydrogen bonds.

In the gas phase, formic acid has two rotamers: the Z and E forms shown in Fig. 1. Both experimental and theoretical studies indicate that the Z rotamer is more stable than the E rotamer by about 4.0 kcal/mol and is therefore about 1000 times more abundant at room temperature [1,2]. The Z rotamer has been well characterized through electron diffraction [3], microwave [4] spectroscopy and infrared spectroscopy [5,6]. The E rotamer has been identified by microwave spectroscopy [1,7].

The structure of formic acid is markedly different in different phases. In the gas phase, formic acid, like glycolic acid [8], forms a cyclic C<sub>2h</sub> dimer with two strong,

nearly linear, equivalent O–H···O H-bonds [4,9,10] shown as F2 in Fig. 1. Like acetic and glycolic acid but unlike many other carboxylic acids whose crystal structures consist of associated dimers, formic acid crystallizes in long catameric chains [11,12] in which H-bonds link each molecule to two neighbors. The low temperature (4.5 K) crystal structure [12] consists of chains of the Z form, whereas at higher temperatures the crystal structure has chains of the E form [11]. The high pressure crystal structure of formic acid was found to contain an arrangement of infinite hydrogen-bonded chains of both the Z and E forms [13]. The infrared spectra of neat liquid formic acid [14] suggest that the predominant forms are chains similar to those observed in the solid.

Hence it is of some interest to determine how many molecules a cluster of formic acid molecules must contain before chain-like structures become energetically favorable. Recent theoretical calculations on formic acid dimers have been carried out using second-order, Møller–Plesset, perturbation theory (MP2) in reasonable basis sets and seven stable dimer structures have been located [15,16]. Computational studies limited to a few structures expected to be among the most stable have been reported for formic acid trimers [17] and tetramers [17,18]. Pentamers have been studied with a model intermolecular potential [17]. Hydrated clusters of formic acid have been studied recently [19].

\* Corresponding author. Fax: +1-506-453-4981.

E-mail address: [ajit@unb.ca](mailto:ajit@unb.ca) (A.J. Thakkar).

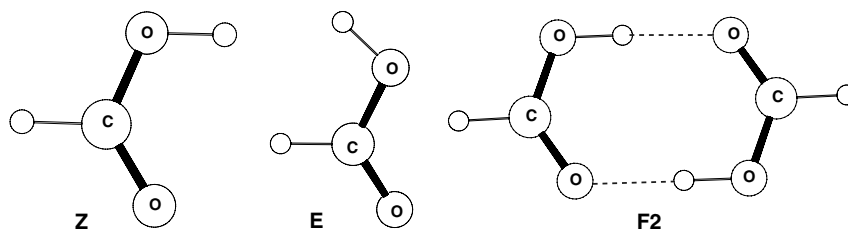


Fig. 1. The Z and E rotamers of formic acid, and the gas-phase dimer structure F2.

In this Letter, we use B3LYP hybrid density functional theory (DFT) calculations with a polarization-consistent, split-valence plus polarization basis set [20] to locate 33 local minima on the potential energy surface of the formic acid trimer. Additional computations are performed for 14 of the lowest-energy structures to assess the sensitivity of the geometries and energies to enlarging the basis set, to varying the hybrid density functional, and to using MP2 rather than DFT calculations. A bond index analysis of these low-lying structures is presented, and used to assess the significance of C–H···O interactions relative to O–H···O H-bonds.

## 2. Methods

DFT computations were made with four different hybrid density functionals based upon the adiabatic connection. These functionals use a mixture of Hartree–Fock exchange and generalized gradient approximations (GGA) for exchange and correlation. Hybrid functionals are expected to be more accurate than pure GGA functionals for hydrogen bonding [24,26]. In particular, we use the B3LYP [21,22], B1LYP [23,24], PBE0 [25], and mPW1PW [26] functionals. Unconstrained geometry optimizations followed by harmonic frequency calculations were carried out with the pc1 and pc2 polarization-consistent basis sets [20]. The pc1 set consists of [3s2p1d/2s1p] contracted Gaussian-type functions (GTF) and has been demonstrated [27] to yield better DFT geometries, frequencies and intensities relative to other polarized, split-valence basis sets. The pc2 set consists of [4s3p2d1f/3s2p1d] contracted GTF and is significantly superior [27] to other polarized, valence triple- $\zeta$  basis sets. Single-point DFT energies were also computed with the polarized, valence quadruple- $\zeta$  pc3 basis set [20] that consists of [6s5p4d2f1g/5s4p2d1f] contracted GTF. The pc1, pc2 and pc3 basis sets for a formic acid trimer contain 156, 354 and 780 contracted GTF, respectively. For all practical purposes, the basis-set limit can be achieved for calculations of geometries and frequencies with the pc2 basis set, and for relative energies with the pc3 basis set. The pc1 and pc2 basis sets have the same size and composition as the cc-pvdz and cc-pvtz correlation-consistent basis sets [28], respectively. The chief difference between the two is

that the correlation-consistent sets are optimized for ab initio calculations that incorporate electronic correlation, whereas the polarization-consistent sets are optimized for DFT calculations.

MP2 geometry optimizations, without any symmetry constraints, followed by frequency computations were carried out using the cc-pvdz basis set [28]. All the DFT and MP2 calculations were performed with the GAUSSIAN 98 suite of programs [29]. Bond orders were computed with the Mulliken–Mayer scheme [30,31] using an in-house program [32].

## 3. Results and discussion

Geometry optimizations were performed at the B3LYP/pc1 level starting from guessed structures. Since the Z rotamer of formic acid is more stable than the E conformation, and the most stable formic acid dimer has both the monomers in the Z conformation, particular attention was paid to guessed trimer structures in which all the monomers were in the Z conformation. This procedure with 52 guessed structures led to 33 unique stationary points all of which were verified to be local minima by frequency analysis.

The 33 B3LYP/pc1 structures can be classified into four types that we call Types D, F, R and C. One group consists of four mostly planar Type D structures in which the lowest-energy dimer is bound to a third formic acid. There are eight mostly planar structures of Type F in which a formic acid monomer is H-bonded to a higher-energy dimer. Another group consists of 11 generally non-planar Type R ring structures held together by three O–H···O H-bonds. Six of these have three O–H···O=C H-bonds, whereas the other five have one or more monomers with their C=O outside the ring and unused for H-bonding. There are 10 mostly planar Type C structures that can be extended into chains. The most stable structure is of Type D and 13 other structures have a relative energy less than 9.8 kcal/mol. The other 19 structures have a relative energy between 10.3 and 22.5 kcal/mol.

The 14 structures with B3LYP/pc1 relative energies less than 10 kcal/mol were reoptimized at the MP2/cc-pvdz, B3LYP/pc2, B1LYP/pc2, PBE0/pc2 and mPW1PW/pc2

levels. Frequency calculations were used to check whether true local minima had been found. Only 13 minima were found with each of these five methods. The B3LYP/pc2 structures are shown in Fig. 2. At the MP2/cc-pvdz level, optimization starting from the cyclic B3LYP/pc1 structure F301 converged to a saddle point. With all the other methods, geometry optimizations starting from two different cyclic B3LYP/pc1 structures (F301 and F352) led to a single minimum (F301). From this point on, we focus

on the 13 structures predicted by all methods using the larger pc2 basis set. Finally, single-point energy calculations with all four DFT methods were carried out at the pc2 geometry using the pc3 basis set.

### 3.1. Geometrical parameters

We begin with a comparison of the B3LYP geometries of the 13 structures obtained with the pc1 and pc2

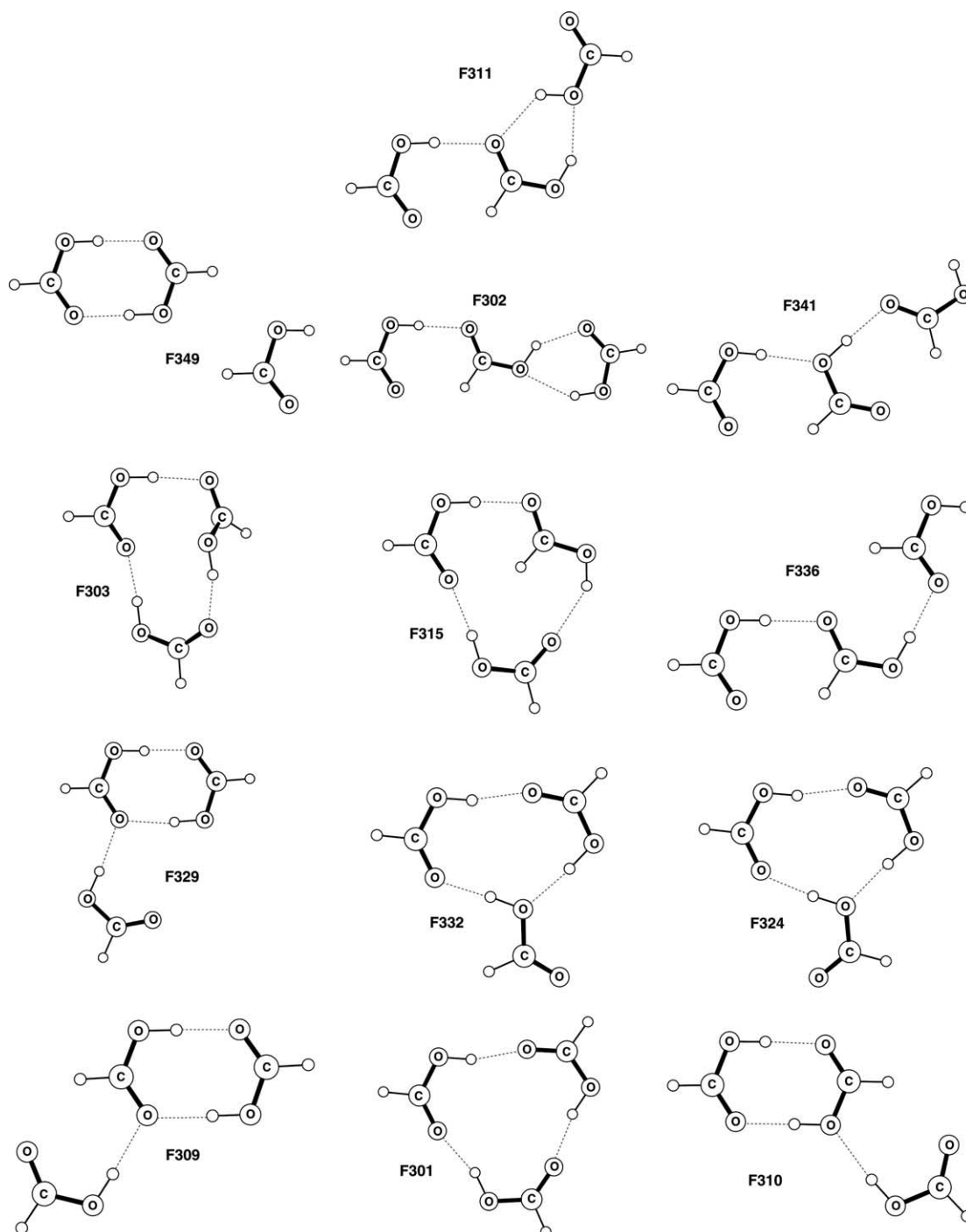


Fig. 2. Low-lying B3LYP/pc2 structures of formic acid trimers. Dashed lines indicate O–H···O hydrogen bonds.

basis sets. The H-bond connectivity pattern remained the same. Three of the 13 structures were non-planar with the pc1 basis set but only two were non-planar with the pc2 basis set. Two B3LYP/pc1 structures (F301 and F329) that were non-planar became planar when the better pc2 basis set was used, whereas the planar F315 became non-planar.

Changing the basis set from pc1 to pc2 changed the intramolecular C–H, C=O, C–O, and O–H bond lengths by an absolute average of 0.7%, 0.5%, 0.1% and 1.1%, respectively. The average change in the intramolecular bond angles was less than 0.3%. However, the H-bond distances increased by an average of 0.038 Å (2.2%) and a maximum of 0.08 Å (4.6%). The H-bond angles changed by an average of 2.0° (1.2%), and a maximum of 12.6° (7.6%) when the basis set was enlarged from pc1 to pc2. Since overly strong binding is characteristic of basis set superposition error (BSSE), we suspect that BSSE is not negligible for the pc1 basis set.

Next we turn to the effect of varying the hybrid density functional with the pc2 basis set. There were no changes in the H-bond patterns or planarity. H-bond lengths generally increased in the order PBE0, mPW1PW, B3LYP, B1LYP. The B3LYP and B1LYP functionals produce relatively close results, as do the PBE0 and mPW1PW functionals. The largest difference among the functionals is that between these two pairs. The H-bond lengths changed by an average of only 0.008 Å or 0.4% when going from PBE0 to mPW1PW, and by an average of 0.013 Å or 0.8% from B3LYP to B1LYP. However, there were average H-bond length differences of 0.035 Å or 2% between mPW1PW and B3LYP. The average changes in the H-bond angles were smaller than 0.8° or 0.5% and less systematic. The later discussion of relative energies shows that all four functionals converge to the same results but the convergence with respect to basis set is fastest for the B3LYP functional. This leads us to believe that the B3LYP/pc2 geometrical parameters are our best converged and probably our most accurate values. A similar lengthening of H-bond lengths with B3LYP relative to PBE0 has been noticed for the dimers of H<sub>2</sub>O and HF [33], and the close similarity between PBE0 and mPW1PW as well as the H-bond contraction in mPW1PW from B3LYP has been reported for malonaldehyde [34].

### 3.2. Relative energies

We now turn to the convergence of the relative energies,  $\Delta E$ , of the 13 structures with respect to the basis set and to the density functional. Table 1 shows that the convergence of the relative energies with respect to basis set is smooth. The relative energies generally decrease by 1–2 kcal/mol when the basis set is enlarged from pc1 to pc2. All 10 methods consistently predict that the F309 structure is the most stable. There is some variation in

the ordering of the less stable structures between the small basis set results, B3LYP/pc1 and MP2/cc-pvdz, and the other eight methods. However, exactly the same ordering is predicted by the B3LYP, B1LYP and mPW1PW functionals with both the pc2 and pc3 basis sets, and by the PBE0 functional with the pc3 set; the PBE0/pc2 ordering is almost the same with just one ordering flip between the F324 and F303 structures. Ramón and Ríos [17] reported MP2 calculations on three trimer structures in a basis set somewhat bigger than pc1 and smaller than pc2. They found F309 to be the most stable, followed by F310 and F301 at relative energies of 1.57 and 1.76 kcal/mol, respectively.

There are significant quantitative variations in  $\Delta E$  with different functionals. The PBE0 and mPW1PW relative energies are usually higher than the corresponding B3LYP and B1LYP energies. With the pc2 basis set, the average absolute difference in  $\Delta E$  relative to the B3LYP results is 0.11, 0.39 and 0.45 kcal/mol for the B1LYP, mPW1PW and PBE0 functionals, respectively. The average absolute difference between the pc2 and pc3 values of  $\Delta E$  is 0.04, 0.11, 0.44 and 0.51 kcal/mol for the B3LYP, B1LYP, mPW1PW and PBE0 functionals, respectively.  $\Delta E$  converges significantly faster with respect to basis set for the B3LYP and B1LYP functionals than for the mPW1PW and PBE0 functionals possibly because BSSE errors are smaller for the former. We expect that the geometrical parameters at the pc2 level, like the relative energies, are best converged for the B3LYP functional. The relative energies are very similar for all the functionals at the pc3 level; the average absolute difference in  $\Delta E$  relative to the B3LYP/pc3 results is only 0.03, 0.07 and 0.07 kcal/mol, respectively, for the B1LYP, mPW1PW and PBE0 functionals.

Next we turn to relative energies including zero-point vibrations  $\Delta E_z$ , relative enthalpies  $\Delta H$ , and relative free energies  $\Delta G$ ; the latter two are for 298.15 K and 1 atm. These energies are listed in Table 2 for all four density functionals using the pc2 basis set. Relative to the B3LYP results, the average absolute differences for the B1LYP, mPW1PW and PBE0 functionals, respectively, are 0.12, 0.41 and 0.48 kcal/mol for  $\Delta E_z$ , 0.12, 0.42 and 0.49 kcal/mol for  $\Delta H$ , and 0.11, 0.26 and 0.38 kcal/mol for  $\Delta G$ . The rank ordering of structures by  $\Delta E_z$  and  $\Delta H$  is exactly the same as that by  $\Delta E$  for the B3LYP, B1LYP and mPW1PW functionals at both the pc2 and pc3 levels. The rank ordering predicted by PBE0/pc2 and PBE0/pc3 is slightly different.

The rank orderings change significantly when  $\Delta G$  is used. All four functionals predict that the cyclic F301 structure becomes the most stable one because of entropy effects. F309 and F329 are the next two most stable structures with close values of  $\Delta G$ . The B3LYP and B1LYP functionals predict that F309 is lower in  $\Delta G$  than F329 whereas the mPW1PW and PBE0 functionals

Table 1

Relative energies,  $\Delta E$ , in kcal/mol for formic acid trimers

	B3LYP pc1	MP2 cc-pvdz	B3LYP pc2	B1LYP pc2	PBE0 pc2	mPW1 pc2	B3LYP pc3	B1LYP pc3	PBE0 pc3	mPW1 pc3
F309	0.00	0.00	0.00	0.00	0.00	0.00	0.00	0.00	0.00	0.00
F301	2.55	—	0.98	0.80	1.74	1.65	1.15	1.13	1.05	1.08
F310	2.35	2.07	2.02	2.01	2.16	2.14	2.01	1.99	1.96	1.96
F329	3.37	2.95	2.63	2.62	2.82	2.67	2.61	2.55	2.55	2.52
F352	3.63	3.09	—	—	—	—	—	—	—	—
F332	5.23	5.92	3.75	3.69	4.35	4.30	3.80	3.75	3.72	3.72
F324	5.16	5.26	3.82	3.73	4.56	4.47	3.89	3.86	3.80	3.79
F303	5.60	5.86	4.27	4.24	4.39	4.57	4.27	4.26	4.22	4.21
F315	6.07	5.84	4.64	4.51	4.82	5.00	4.63	4.59	4.56	4.56
F336	6.42	5.99	5.19	5.02	5.64	5.53	5.23	5.19	5.12	5.14
F349	7.86	7.24	6.33	6.27	6.72	6.47	6.24	6.24	6.19	6.20
F302	8.75	7.98	7.47	7.29	8.14	8.01	7.42	7.39	7.35	7.35
F341	9.75	8.74	8.27	8.03	9.04	8.89	8.31	8.27	8.21	8.21
F311	9.62	8.62	8.57	8.34	9.41	9.28	8.58	8.54	8.48	8.48

mPW1 stands for mPW1PW.

Table 2

Relative energies in kcal/mol obtained with the pc2 basis set

	B3LYP			B1LYP			PBE0			mPW1PW		
	$\Delta E_z$	$\Delta H$	$\Delta G$	$\Delta E_z$	$\Delta H$	$\Delta G$	$\Delta E_z$	$\Delta H$	$\Delta G$	$\Delta E_z$	$\Delta H$	$\Delta G$
F309	0.00	0.00	1.40	0.00	0.00	1.57	0.00	0.00	1.35	0.00	0.00	1.14
F301	0.43	0.87	0.00	0.23	0.65	0.00	1.17	1.67	0.00	1.09	1.57	0.00
F310	1.71	1.82	2.69	1.71	1.82	2.85	1.82	1.91	2.76	1.80	1.90	2.49
F329	2.22	2.49	1.42	2.21	2.47	1.78	2.41	2.69	1.08	2.27	2.53	0.78
F332	3.19	3.46	3.87	3.13	3.40	3.97	3.83	4.11	4.39	3.78	4.05	4.17
F324	3.26	3.55	3.61	3.17	3.45	3.70	4.01	4.32	4.16	3.93	4.23	3.89
F303	3.81	3.88	5.60	3.77	3.85	5.69	3.95	4.00	5.75	4.13	4.19	5.72
F315	4.41	4.66	5.65	4.26	4.50	5.67	4.62	4.89	5.76	4.79	5.06	5.71
F336	4.84	5.22	5.25	4.64	5.01	5.22	5.38	5.77	5.79	5.24	5.64	5.36
F349	5.43	6.00	3.79	5.38	5.94	3.94	5.83	6.40	4.24	5.54	6.15	3.14
F302	6.92	7.36	6.55	6.70	7.14	6.48	7.69	8.13	7.26	7.52	7.98	6.82
F341	7.64	8.17	7.62	7.37	7.90	7.54	8.51	9.06	8.45	8.32	8.88	7.97
F311	7.98	8.49	7.48	7.72	8.22	7.43	8.92	9.45	8.11	8.74	9.28	7.57

predict the opposite. The F349 structure in which a formic acid dimer is held to the third monomer by two weak C–H···O interactions climbs four steps higher in the rank ordering when  $\Delta G$  is considered.

### 3.3. Qualitative aspects

We now turn to a qualitative discussion of the 13 structures shown in Fig. 2. There are five ring structures (F301, F332, F324, F303, F315). Two of these (F332, F324) contain a monomer with unused H-bonding capability. Three (F332, F303, F315) contain a monomer in the higher-energy E conformation. Two (F303, F315) are non-planar. The F301 structure has three strong, nearly equivalent O–H···O=C H-bonds in a planar ring connecting three monomers in the Z conformation. All the H-bond distances in this complex are 1.72 Å, the H-bond angles lie in the narrow range of 163.8°–165.7°, and all the H-bond orders are

0.1 as seen from Table 3 which lists the orders, lengths and angles of the O–H···O H-bonds in the 13 B3LYP/pc2 structures in a clockwise manner starting from the top left. F315 has much greater variation in H-bond lengths and orders than F301 and has two endocyclic C–H···O bonds. There are very strong H-bonds with orders ranging from 0.11 to 0.15 in F303 but non-planarity and a strong distortion of one of the monomers toward the E conformation make F303 a less stable structure than F301.

F309, F310, F329 and F349 are planar structures of Type D. The least stable of these is F349 in which the third formic acid forms no O–H···O H-bonds and is held to the dimer by two weak C–H···O interactions. In F329 the third monomer forms only one O–H···O H-bond to the dimer, whereas in F309 and F310 it forms both an O–H···O and an C–H···O bond. For the 13 clusters under consideration, O–H···O bonds have orders between 0.036 and 0.179 with an average

Table 3  
H-bond parameters for the 13 most stable trimers at the B3LYP/pc2 level

Trimer	Order	Length	Angle	Order	Length	Angle	Order	Length	Angle
F309	0.165	1.660	179.2	0.114	1.721	177.5	0.081	1.802	177.8
F301	0.099	1.724	163.8	0.098	1.721	165.7	0.099	1.720	165.3
F310	0.150	1.679	177.2	0.054	1.902	174.8	0.179	1.634	179.0
F329	0.175	1.630	179.6	0.093	1.797	173.0	0.075	1.820	176.7
F332	0.107	1.706	168.9	0.103	1.752	174.7	0.146	1.665	178.4
F324	0.099	1.740	167.3	0.096	1.747	176.4	0.132	1.688	171.2
F303	0.146	1.718	174.4	0.117	1.711	164.9	0.108	1.716	172.9
F315	0.171	1.673	176.0	0.043	1.987	145.1	0.078	1.793	174.3
F336	0.115	1.738	179.3	0.118	1.741	178.1	–	–	–
F349	0.153	1.674	177.9	0.160	1.667	178.4	–	–	–
F302	0.110	1.766	176.8	0.099	1.841	143.1	0.036	2.114	145.2
F341	0.065	1.859	177.2	0.123	1.730	177.4	–	–	–
F311	0.086	1.805	176.4	0.048	2.031	131.5	0.054	1.955	152.0

The parameters for each structure are listed in a clockwise manner starting from the top-left H-bond. Lengths and angles in Angstroms and degrees, respectively.

of 0.108 whereas C–H···O interactions have substantially smaller bond orders between 0.010 and 0.022 with an average of 0.017. O–H···O=C bonds are often, but not invariably, stronger than O–H···O–H bonds.

F336 and F341 are planar, chain-type structures with the former more stable because both its H-bonds are relatively strong. These chain-like structures are energetically unfavorable, and presumably become stabilized only in larger clusters. F302 and F311 are relatively high-energy, planar structures of Type F which can be extended in chain-like fashion only at one end unlike the true chain structures F336 and F341 that can be extended at both ends.

#### 4. Concluding remarks

33 local minima on the potential energy surface of the formic acid trimer were identified at the B3LYP/pc1 level. Many additional computations were performed with larger basis sets and four hybrid density functionals for the 13 lowest structures. The B3LYP and B1LYP functionals converge faster with basis set than the mPW1PW and PBE0 functionals, possibly because of lower sensitivity to basis set superposition errors.

Energies, with and without zero-point corrections, and enthalpies all identify the most stable structure as F309 which consists of a monomer H-bonded to the lowest-energy dimer. However, when Gibbs free energies are considered, all methods find the planar, symmetric, ring structure F301 to be the most stable.

The trimer structures reported here could be a valuable test of intermolecular potential functions for formic acid [16,17,35]. Structural studies of larger clusters of four, five and six formic acid molecules are being carried out in our laboratory.

#### Acknowledgements

We thank Emil Proynov for useful discussions. This work was supported by the Natural Sciences and Engineering Research Council of Canada.

#### References

- [1] W.H. Hocking, Z. Naturforsch. 31A (1976) 1113.
- [2] M. Pettersson, J. Lundell, L. Khriachtchev, M. Räsänen, J. Am. Chem. Soc. 119 (1997) 11715.
- [3] J. Karle, L.O. Brockway, J. Am. Chem. Soc. 66 (1944) 574.
- [4] G.H. Kwei, R.F. Curl Jr., J. Chem. Phys. 32 (1960) 1592.
- [5] R.C. Millikan, K.S. Pitzer, J. Chem. Phys. 27 (1957) 1305.
- [6] I.C. Hisatsune, J. Heicklen, Can. J. Spectrosc. 18 (1973) 135.
- [7] E. Bjarnov, W.H. Hocking, Z. Naturforsch. 33A (1978) 610.
- [8] N.E.-B. Kassimi, E.F. Archibong, A.J. Thakkar, J. Mol. Struct. (Theochem) 591 (2002) 189.
- [9] A. Almenningsen, O. Bastiansen, T. Motzfeldt, Acta Chem. Scand. 23 (1969) 2848.
- [10] A. Almenningsen, O. Bastiansen, T. Motzfeldt, Acta Chem. Scand. 24 (1970) 747.
- [11] I. Nahringsbauer, Acta Crystallogr. B 34 (1978) 315.
- [12] A. Albinati, K.D. Rouse, M.W. Thomas, Acta Crystallogr. B 34 (1978) 2188.
- [13] D.R. Allan, S.J. Clark, Phys. Rev. Lett. 82 (1999) 3464.
- [14] P. Waldstein, L.A. Blatz, J. Phys. Chem. 71 (1967) 2271.
- [15] L. Turi, J. Phys. Chem. 100 (1996) 11285.
- [16] W. Qian, S. Krimm, J. Phys. Chem. A 105 (2001) 5046.
- [17] J.M.H. Ramón, M.A. Ríos, Chem. Phys. 250 (1999) 155.
- [18] M. Stein, J. Sauer, Chem. Phys. Lett. 267 (1997) 111.
- [19] D. Wei, J.-F. Truchon, S. Sirois, D. Salahub, J. Chem. Phys. 116 (2002) 6028.
- [20] F. Jensen, J. Chem. Phys. 116 (2002) 7372.
- [21] A.D. Becke, J. Chem. Phys. 98 (1993) 5648.
- [22] P.J. Stephens, F. Devlin, C. Chabalowski, M. Frisch, J. Phys. Chem. 98 (1994) 11623.
- [23] A.D. Becke, J. Chem. Phys. 104 (1996) 1040.
- [24] C. Adamo, V. Barone, Chem. Phys. Lett. 274 (1997) 242.
- [25] J.P. Perdew, K. Burke, M. Ernzerhof, Phys. Rev. Lett. 77 (1996) 3865.
- [26] C. Adamo, V. Barone, J. Chem. Phys. 108 (1998) 664.
- [27] F. Jensen, J. Chem. Phys. 118 (2003) 2459.

- [28] T.H. Dunning Jr., J. Chem. Phys. 90 (1989) 1007.
- [29] M.J. Frisch et al., GAUSSIAN 98, Revision A.11, Gaussian Inc., Pittsburgh, PA, 2001.
- [30] I. Mayer, Chem. Phys. Lett. 97 (1983) 270.
- [31] I. Mayer, Int. J. Quantum Chem. 29 (1986) 477.
- [32] A.J. Thakkar, Gbondo (1995).
- [33] E. Proynov, H. Chermette, D.R. Salahub, J. Chem. Phys. 113 (2000) 10013.
- [34] C. Adamo, V. Barone, J. Chem. Phys. 110 (1999) 6158.
- [35] P. Jedlovsky, L. Turi, J. Phys. Chem. A 101 (1997) 2662.